The FASEB Journal express article 10.1096/fj.01-0691fje. Published online December 28, 2001.

Disruption of the taurine transporter gene (*taut*) leads to retinal degeneration in mice

Birgit Heller-Stilb*[,§], Claudia van Roeyen*[,§], Kristina Rascher[†], Hans-Georg Hartwig[†], Andrea Huth[‡], Mathias W. Seeliger[‡], Ulrich Warskulat*, and Dieter Häussinger*

*Department of Gastroenterology, Hepatology and Infectiology, Heinrich Heine University Düsseldorf, Germany; [†]Department of Anatomy, Heinrich Heine University Düsseldorf, Germany; and [‡]Retinal Electrodiagnostics Research Group, Department of Ophthalmology, University of Tübingen, Germany. [§]These authors contributed equally to this work.

Corresponding author: Dieter Häussinger, Department of Gastroenterology, Hepatology, and Infectiology, Heinrich Heine University, Moorenstrasse 5, D-40225 Düsseldorf.
E-mail: haeussin@uni-duesseldorf.de

ABSTRACT

Taurine is involved in cell volume homeostasis, antioxidant defense, protein stabilization, and stress responses. High levels of intracellular taurine are maintained by a Na^+-dependent taurine transporter (TAUT) in the plasma membrane. In view of the immunomodulatory and cytoprotective effects of taurine, a mouse model with a disrupted gene coding for the taurine transporter (*taut*-/- mice) was generated. These mice show markedly decreased taurine levels in a variety of tissues, a reduced fertility, and loss of vision due to severe retinal degeneration. In particular, the retinal involvement identifies the taurine transporter as an important factor for the development and maintenance of normal retinal functions and morphology.

Key words: knockout mice • compatible organic osmolytes • retinitis pigmentosa

Taurine is the most abundant amino acid in many tissues and, depending on the species, intracellular concentrations of 10–70 mmol/l are found in mammalian heart, brain, neutrophils, skeletal muscle, liver, and retina (1–4), whereas taurine concentrations in extracellular fluids reach only 20–100 μmol/l in humans (1, 5), but in mice up to 600–800 μmol/l (6, 7). The zwitterionic nature of taurine prevents its passage through lipid layers and allows the Na^+-dependent taurine transport system (TAUT) to build up very steep concentration gradients between cellular and extracellular spaces. *taut* belongs to the sodium- and chloride-coupled transporter gene family that is also known as the neurotransmitter transporter gene family (8, 9). TAUT is found in many tissues and has been cloned from various species with remarkable sequence similarity (10–14). In most tissues, TAUT expression is regulated osmotically, a finding in good agreement with the importance of taurine as an organic osmolyte (15–17). Apart from cell volume regulation, taurine may act as a neuromodulator and can protect cells *in vitro* against various types of injury (1–4, 18–20). The underlying mechanisms are not yet well understood but may involve antioxidant effects (1–3), modulation of intracellular calcium levels and ion channel activities (1), membrane and protein stabilization (1, 17, 19), and modulation of immune (3, 20–22) and stress responses (18). In view of the multiple roles attributed to

intracellular taurine and its transport, we created a TAUT-deficient murine model by gene knockout.

MATERIALS AND METHODS

Mice

The *taut* knockout mice were generated by homologous recombination and had a mixed genetic background (C57Bl/6 × 129/SvJ). Animals were housed in isolators at a 12–12 h light–dark cycle, according to the rules of the local ethical guidelines.

Screening of the recombinant embryonic stem cells

We extracted DNA by using the QIAamp mini kit (Qiagen, Hilden, Germany). For the polymerase chain reaction (PCR) identification of homologous recombinated embryonic stem (ES) cell clones, we used the primers neoK2 2A (5'-TCTGGATGCACCCGAGTGACTAAGG) and neoK2 2B (5'-AATATGCGAAGTGGACCTGGGACC), which generated a product of 2100 bp. PCR conditions were 5 min at 94˚C, followed by 35 cycles with 1 min at 94°C, 1 min at 60°C, and 2.5 min at 72°C. Samples were electrophoresed in a 1.5% agarose gel.

Genotyping of the knockout mouse

We extracted DNA from tail tissue by using the DNeasy Tissue Mini Kit (Qiagen, Hilden, Germany). The DNA was analyzed by PCR (5 min at 94°C followed by 35 cycles of 1 min at 94°C, 57°C, and 72°C, respectively, with 8 min extension time at 72°C on cycle 35). Wild-type mice were identified with the primer pairs taut-neo2 (5`-CAGGGTATACCTGGACTGGG) and neo2 (5`-GACAGAATAAAACGCACGGG). The primers taut-Ex1.2 (5'-AAGCCTTCTCCAGGGAAGAG) and taut-Ex1r (5`-CCACAGACAGCACAAAGTC), which amplified the exon 1 of the *taut* gene, were used for differentiating between (*taut* +/-) and (*taut* -/-) animals. In all PCR reactions exon 2 of *taut* was amplified simultaneously by using primers TEx25/2 (5`-CGTCATTGTGTCCCTCCTG) and taut-Ex2r (5`-TGAGGTGAAGTTGGCAGTGCT) as an internal control.

Northern-blot analysis

Total RNA from liver and kidney of wild-type and knockout mice was isolated by using the RNeasy Midi Kit (Qiagen, Hilden, Germany). Northern blotting and hybridization using a *taut* exon 1 probe (corresponding to bp 231 to 393 of the mus cookii *taut* sequence, Genbank Acc. No. L03292) were carried out under high stringency conditions according to standard protocols as previously described (23).

In vitro transcription/translation

Total RNA was reverse-transcribed by using a first-strand cDNA synthesis kit (Roche, Mannheim, Germany). The complete coding sequence of the *taut* gene (1932 bp) was amplified by using the primers 5`taut (5`-GCTAATACGACTCACTATAGGAACAGACCACCGAACCAGTGCCACAGCC) and 3`taut (5`-CAACATGGCCCGGACCTCAC). PCR was performed with the Expand Long Template PCR System (Roche). PCR conditions were 94°C for 2 min, 10 cycles at 94°C for 10 sec, 62°C

for 30 sec, and 68°C for 2 min, 20 cycles at 94°C for 10 sec, 62°C for 30 sec, 68°C for 2 min plus an extension for 20 sec for each cycle, and a final extension at 68°C for 7 min. For the *in vitro* transcription and translation, we used the TNT T7 quick-coupled transcription/translation system (Promega, Mannheim, Germany) according to the manufacturer's protocol.

Measurement of taurine transport into primary fibroblasts

Freshly removed muscles of the hind leg from 2–4 month old mice were diced and cultivated in Dulbecco's modified Eagle medium supplemented with 4.5 mg/l glucose, 15% fetal bovine serum, nonessential amino acids, and 100 µg/ml gentamycin and fungizone. Fibroblasts began to grow out of the tissue after 2–3 days and were cultured for 17–27 days. The uptake of taurine (200 µM in medium) into fibroblasts was then measured over an 8-h period as described previously (23).

Determination of taurine levels in tissues and plasma

Freshly removed tissues and plasma were frozen in liquid nitrogen and then stored at –70° C. Before freezing, the lenses and vitreous bodies were eliminated from the eyes. Frozen tissue was homogenized by using a microhomogenizer and was weighed five times without thawing. Proteins were removed by incubation in 10% sulfosalicylic acid on ice for 1 h. After centrifugation (10 min at 21,000 x g), the lipids were extracted with dichloromethane from the supernatant. Plasma was added to an equal amount of 10% sulfosalicylic acid. Taurine content was analyzed in a BioChrom20 amino acid analyzer (Amersham-Pharmacia, Freiburg, Germany).

Morphological examination of the retina

The mice were anesthesized in ether or killed with CO_2 before decapitation. The eyes were excised rapidly and fixed by immersion in a mixture of 4% paraformaldehyde/2.5% glutardialdehyde containing 0.01 mM $CaCl_2$ for 24 h. The lenses were then removed and the specimens were rinsed in 0.1 M phosphate buffer (pH 7.4) before postfixation in 1% OsO_4 for 3 h at 4°C. Following dehydration in ethanol, the tissue was embedded in Epon. Semithin sections were stained with toluidine blue. Ultrathin sections were cut with a diamond knife and contrasted with uranyl acetate/lead citrate before viewing in a Hitachi EM600 (Tokyo, Japan). At least five wild-type and five knockout mice in the following age groups were examined: 2–4 wk, 2–6 months, 7–12 months, and older animals.

Electroretinograms

Electroretinograms (ERGs) were obtained according to previously described procedures (24). In summary, mice were dark-adapted overnight and their pupils were dilated. Anesthesia was induced by subcutaneous injection of ketamine (66.7 mg/kg), xylazine (11.7 mg/kg), and atropine (1 mg/kg). Silver needle electrodes served as reference (forehead) and ground (tail), and rings made from 0.5 mm ∅ gold wire as monopolar corneal electrodes. The ERG equipment consisted of a Ganzfeld bowl, a DC amplifier, and a PC-based control and recording unit (Toennies Multiliner Vision, Jaeger/Toennies, Höchberg, Germany). Band-pass filter cut-off frequencies were 0.3 and 300 Hz. Stimulus intensities were increased from 10^{-4} cd*s/m^2 to 25

cd*s/m^2, divided into 10 steps of 0.5 and 1 log cd*s/m^2. Ten subsequent responses were averaged with an inter-stimulus interval of 5 sec or 17 sec (for 1, 3, 10, 25 cd*s/m^2).

Detection of apoptosis by TUNEL assay

Retinal sections were deparaffinized with xylene and rehydrated in a graded series of ethanol to destillated water. The terminal deoxynucleotidyltransferase-mediated dUTP nick-end labeling (TUNEL) assay was then carried out with an *in situ* cell death detection kit (Roche) (25). The incorporated fluorescein was detected by measuring the cell-associated fluorescence. The excitation wavelength was 490 nm.

Statistics

Data are expressed as mean ± SEM (*n*=number of cell preparations from different animals).

RESULTS

Targeted disruption of the *taut* gene

We isolated an 18-kb XhoI genomic clone from a λ phage library containing mouse strain 129SvJ genomic DNA by screening with a cDNA *taut* probe. To disrupt the *taut* locus, we designed an isogenic targeting vector to delete exon 1 of *taut* (Fig. 1a). ES cells (derived from 129/SvJ strain, Genomesystems, St. Louis, MO) were electroporated with the linearized vector and, after 48 h, colonies underwent positive–negative selection with geneticin (400 µg/ml for the first 4 days, then 250 µg/ml) and gancyclovir (2 µM) (26). Double-resistant clones were screened for the desired homologous recombination by PCR. We analyzed PCR-positive clones by Southern blot hybridization to verify that a single integration had taken place by homologous recombination (data not shown). Two ES clones containing the targeting event were injected into blastocysts of C57BL/6 mice to produce chimeras (RCC, Füllinsdorf, Switzerland). Only one ES clone transmitted the *taut* mutation through the germ line. Heterozygous (*taut*+/-) mice with a C57BL/6 × 129/SvJ background were intercrossed to produce wild-type (*taut*+/+), heterozygous (*taut*+/-), and homozygous (*taut*-/-) animals in the F2 progeny. Offspring of matings between (*taut*+/-) females and (*taut*+/-) males were observed in 14 of 16 matings. The offspring showed a normal Mendelian ratio, suggesting there was no specific embryonic lethality in the mutants. Of the 13 (*taut*+/-) females, 6 became pregnant with (*taut*-/-) males, but none of 5 (*taut*-/-) females became pregnant with (*taut*+/-) males. Only 4 of 21 different breeding pairs of (*taut*-/-) mice produced offspring, but all 4 matings occurred between (*taut*+/+) females and (*taut*-/-) males.

Characterization of the *(taut-/-)* mouse

(*taut*-/-) mice exhibited a lower body mass compared with (*taut*+/-) and wild-type mice (Table 1). Offspring were characterized by PCR. In (*taut*-/-) mice, a fragment of the targeting construct was amplified in PCR1, whereas exon 1 was detected by PCR2 in wild-type (*taut*+/+) mice (Fig. 1b).

The deletion of exon 1 of the *taut* gene led to a truncated protein of 450 amino acids (wild-type: 621) as shown in the *in vitro* transcription and translation assay (Fig. 1c). Transmembrane domains 1 to 3 and part of the large extracellular region of the protein were no longer present.

(*taut*-/-) and (*taut*+/+) mice were compared by Northern blot analysis. No expression of the *taut* exon 1 was found in either kidney or liver tissue of (*taut*-/-) animals, whereas wild-type mice showed exon 1 expression in both organs (Fig. 1d).

Loss of TAUT function in the null mutation was verified by measuring taurine uptake by fibroblasts *in vitro*. When primary fibroblasts were exposed to medium supplemented with 200 µM taurine for 8 h, taurine uptake into fibroblasts isolated from (*taut*-/-) mice was 98% lower (4.2 $\pm$ 1.3 nmol/mg protein, n=3) than normal (201.7 $\pm$ 37.0 nmol/mg protein, n=5).

(*taut*-/-) mice showed remarkably low taurine levels when compared with wild-type mice. A reduction of taurine concentration by about 74% was observed in plasma, kidney, liver, and eye (Table 2). In skeletal and heart muscle, taurine concentrations were even decreased about 97%.

Retinal degeneration in (*taut*-/-) mice

The most prominent morphological feature of (*taut*-/-) mice was severe and progressive retinal degeneration (Fig. 2). In contrast to retinas of wild-type mice (Figs. 2a, b and 3a), no photoreceptor outer or inner segments were discernible light microscopically in (*taut*-/-) mice beyond an age of 4 wk (Fig. 2d–h). In 2-wk-old (*taut*-/-) mice, the outer nuclear layer (ONL) was largely preserved (Figs. 2c and 3b, c), but the outer and inner photoreceptor segments were much smaller when compared with those of 2-wk-old wild-type animals (Fig. 2b). At 1–2 months of age, only one to three layers of nuclei were seen in the ONL (Fig. 2d, e), and this layer had disappeared completely in older animals (Fig. 2f–h).

Electron microscopic examination of retinas from (*taut*-/-) mice at 1–2 months revealed advanced stages of photoreceptor cell degeneration: many of the remaining nuclei were pyknotic, but ribbon synapses as well as remnants of outer segment disks occasionally were visible (Fig. 3c–e).

Ultrastructural examination of knockout mice older than 2 months showed that the neurons of the inner nuclear layer (INL) were separated from the pigment epithelium (PE) by thin lamellae resembling Müller cell processes (Fig. 3f). The INL was irregular in advanced stages of degeneration and varied in thickness from only a few cells at the PE to large groups of cells extending from the PE through the inner plexiform layer into the ganglion cell layer (Fig. 2g, h). The latter layer appeared to be intact, but may have fewer cells than in wild-type mice.

The effect of taut activity loss on retinal function was assessed with ERG. A functional evaluation of 6-week to 4-month-old mutants showed that the ERG was absent completely in (*taut* -/-) mice (Fig. 4c), whereas that of the heterozygous mice was not different from normal (data not shown). However, a developmental study of (*taut*-/-) mice at ages between 2 and 4 wk revealed some small, but distinct remaining electrical activity (Fig. 4b) both at low and high stimulus intensities. Compared with the controls, the b-wave amplitude of the ERG increased only insignificantly from postnatal week 2 to 3 and decreased rapidly thereafter (Fig. 4d–f).

Nevertheless, the double-peaked amplitude versus intensity curves (Fig. 4d, e) implicate that both rod and cone systems are somewhat functional. To assess whether the functional loss observed may be due simply to the failure of the (*taut* -/-) mice to gain weight normally after birth, the b-wave amplitude obtained at a certain stimulus intensity (3 cds/m²) was related to age and body weight (Fig. 4g). It was found that although the mutants indeed trailed the controls of the same age in weight during postnatal development (open and filled symbols in Fig. 4g), the ERG of controls of comparable weight—regardless of the age—was much larger in all cases, thus excluding a major impact of that parameter.

Detection of apoptosis in the retina of *(taut-/-)* mice

We analyzed the retinas of 2- and 6-wk-old (*taut*-/-) mice for apoptosis by using the TUNEL assay. TUNEL-positive nuclei were present consistently in the (*taut*-/-) animals. (*taut* -/-) mice display deterioration of inner and outer photoreceptor segments and a progressive reduction of ONL thickness from postnatal day 14 through 6 wk, where a single row of condensed photoreceptor nuclei was observed (Fig. 5). We saw no such nuclei in our retinal sections from age-matched wild-type mice.

DISCUSSION

As shown in this study, homozygous disruption of exon 1 of the *taut* gene results in plasma hypotaurinemia, a 98% decrease in taurine uptake by primary fibroblasts and low levels of taurine in all tissues examined. These findings suggest that defective taurine uptake due to disruption of *taut* cannot be compensated by taurine uptake via other transport systems such as the amino acid transport system A. We found a 98%–99% decrease of tissue taurine levels in heart and skeletal muscle, whereas liver and kidney taurine levels were lower than in wild-type mice by only about 70%–80%. The liver is known to be a major site of taurine synthesis (27), and it seems likely that this may at least partially compensate for disrupted TAUT function in this organ.

(*taut*-/-) mice exhibited a marked impairment of reproduction. Although taurine is not used for protein synthesis, it is normally present in high concentrations in mouse eggs and oviductal and uterine fluid and acts as an osmolyte in mouse oocytes and embryos (28) and promotes embryo development in a variety of species, including mouse (29) and humans (30). Taurine is also present in human semen, the sperm acrosome (31), and maintains sperm motility (32) necessary for optimal fertilization. These roles of taurine at various levels of reproduction may well explain the reduced fertility of (*taut*-/-) mice. However, TAUT is apparently much more crucial for fertility in females than in males, because offspring were born when male (*taut*-/-) mice mated with (*taut*+/-) or wild-type females, whereas (*taut*-/-) females show reduced fertility regardless of the *taut* status of the male partner.

Another prominent feature of (*taut*-/-) mice is severe and progressive retinal degeneration. The taurine levels were diminished about 74% in eyes from 12-day-old (*taut*-/-) mice when compared with those from wild-type mice. At 2 wk postnatal, the usual age of eye opening, an approximately equal number of rows of photoreceptor nuclei in mutants and wild-type mice were still apparent. Inner and outer photoreceptor segments in the mutants were clearly distinguishable but were already smaller than in the controls. Retinal function was also observable at that stage,

with amplitudes reduced to about one-third of those of age-matched controls. One week later, ERG amplitudes had dropped to 10%–15% of normal. At one month of age, the number of photoreceptor cell nuclei was reduced markedly. In light microscopy, photoreceptor segments were largely absent, and only remnants of photoreceptor disks and synapses were found at the ultrastructural level. The ERG, even to bright stimuli, was close to noise level and the further morphological deterioration was paralleled by a complete loss of retinal function. These findings indicate that photoreceptor cells initially develop but then undergo degeneration.

It has been recognized recently that programmed cell death is a crucial aspect in a variety of human and animal retinal dystrophies (33, 34). Apoptosis apparently is also involved in retinal degeneration in the (*taut-/-*) mouse, because no macrophages were found in the subretinal space and the photoreceptor cell nuclei were TUNEL-positive. In all mammalian species examined so far, high taurine concentrations were found in the retina, with about two-thirds of retinal taurine being localized in the photoreceptor layer (1, 35). The absence of taurine as a radical scavenger may accelerate programmed cell death. However, additional mechanisms may also be involved, because retinal degeneration was also inducible by taurine deficiency in light-deprived cats (36). In addition to its role as an osmoregulator and antioxidant, taurine has trophic effects on the retina and modulates visual signal transduction at the level of Ca^{2+} transport and protein phosphorylation (1, 35, 37).

The lack of light-induced retinal function and the marked morphological changes in (*taut-/-*) mice underline the importance of an intact taurine transport system for the photoreceptor cells. Studies in cats (for which taurine is an essential amino acid) have shown that an acquired deficiency in taurine leads to progressive retinal degeneration of the cone-rod type (36). Because neither the rod nor the cone system in our (*taut-/-*) mice was found to respond to light stimulation at the ages tested, an assessment of differential effects of the mutation on these two systems was not feasible.

The importance of taurine for retinal function is underlined by the fact that ERGs are abnormal in cases of human taurine deficiency caused by long-term parenteral nutrition (38). Cats are dietary dependents with regard to taurine. ERGs were also abnormal in cats fed taurine-deficient diets and outer segment structure was severely disturbed (36, 39). Mice are not dietary dependents, but their photoreceptor cells are dependent evidently on an intact taurine transport system for maintaining structurally and functionally sufficient levels of intracellular taurine. The effects of disrupted taurine transport in the retina have been examined in animals treated with guanidinoethyl sulfonate (GES), an antagonist of taurine uptake (40, 41). Some aspects of retinal degeneration in our (*taut-/-*) mouse closely resemble those described in the GES-treated rats, particularly with respect to disruption of outer segment disks and ultimate loss of photoreceptor cells. Deficits in the ERGs of GES-treated rats (42) were also comparable with those seen in the *taut* knockout mice. It remains to be determined whether retinal dystrophy in (*taut-/-*) mice is caused directly by a lack of taurine or whether taurine transport deficiency leads to disturbances in the osmotic balance specific to photoreceptor cells.

Human retinitis pigmentosa (RP) is a genetically heterogeneous group of hereditary retinal dystrophies (43, 44). RP is characterized by the progressive degeneration and loss of retinal cells and represents, with an incidence of about 1:4,000, the most common cause of inherited blindness in the adult. So far, 23 distinct chromosomal loci have been recognized, but in only 12

of them have the causative genes and mutations been identified. The most common mutations leading to RP involve the genes for rhodopsin, different rod cGMP phosphodiesterase subunits and peripherin. No mutated genes affecting taurine transport or metabolism have been identified so far. Nonetheless, longstanding and ongoing debate focuses on the role of taurine in RP (35, 45). Although taurine supplementation in RP patients did not lead to any significant clinical improvement (35), there are reports on reduced taurine uptake into platelets and lymphoblastoid cells as well as extremely decreased plasma taurine levels in some RP patients (45, 46). Thus, the present study suggests that *taut* might be another candidate gene whose mutation may underly RP in a subgroup of patients.

ACKNOWLEDGMENTS

The λ phage library containing mouse strain 129/SvJ genomic DNA was a kind gift from W. Schrader, Düsseldorf). The authors are grateful to I. Mönnighoff for determining taurine levels. Expert electron microscopy was done by G. Servos and technical assistance was provided by G. Berthold. This study was supported by the Fritz-Thyssen-Stiftung and through SFB 575 "Experimentelle Hepatologie" (Düsseldorf).

REFERENCES

1. Huxtable, R. J. (1992) Physiological actions of taurine. *Physiol. Rev.* **72**, 101–163

2. Timbrell, J. A., Saebra, V., and Waterfield, C. J. (1995) The in vivo and in vitro protective properties of taurine. *Gen. Pharmac.* **26**, 453–462

3. Green, T. R., Fellman, J. H., Eicher, A. L., and Pratt, K. L. (1991) Antioxidant role and subcellular localization of hypotaurine and taurine in human neutrophils. *Biochim. Biophys. Acta* **1073**, 91–97

4. Chapman, R. A., Suleiman, M. S., and Earm, Y. E. (1993) Taurine and the heart. *Cardiovascular Res.* **27**, 358–363

5. Vom Dahl, S., Mönnighoff, I., and Häussinger, D. (2000) Decrease of plasma taurine in Gaucher disease and its sustained correction during enzyme replacement therapy. *Amino Acids* **19**, 585–592

6. Komaroy, A. M. and Reddy, M. N. (1998) Effect of septic shock on nitrate, free amino acids and urea in murine plasma and urine. *Clin. Biochem.* **31**, 107–111

7. Kontro, P., Marnela, K. M., and Oja, S. S. (1984) GABA, taurine and hypotaurine in developing mouse brain. *Acta Physiol. Scand.* **537**, 71–74

8. Kwon, M. H. and Handler, J. S. (1995) Cell volume regulated transporters of compatible osmolytes. *Curr. Biology* **7**, 465–471

9. Schloss, P., Puchel, A. W., and Betz, H. (1994) Neurotransmitter transporters: new members of known families. *Curr. Op. Cell. Biol.* **4**, 595–599

10. Uchida, S., Kwon, H. M., Yamauchi, A., Preston, A. S., Marumo, F., and Handler, J. S. (1992) Molecular cloning of the cDNA for an MDCK cell Na^+ - and Cl^- -dependent taurine transporter that is regulated by hypertonicity. *Proc. Natl. Acad. Sci. USA* **89**, 8230–8234

11. Smith, K. E., Borden, L. A., Wang, C. D., Hartig, P. R., Branchek, T. A., and Weinshank, R. L. (1992) Cloning and expression of a high affinity taurine transporter from rat brain. *Mol. Pharmacol.* **42**, 563–569

12. Liu, Q. R., Lopez-Corcuera, B., Nelson, H., Mandian, S., and Nelson, N. (1992) Cloning and expression of a cDNA encoding the transporter of taurine and ß-alanine in mouse brain. *Proc. Natl. Acad. Sci. USA* **89**, 12145–12149

13. Vinnacota, S., Qian, X., Egal, H., Sarthy, V., and Sarkar, H. K. (1997) Molecular characterization and in situ localization of a mouse retinal taurine transporter. *J. Neurochem.* **69**, 2238–2250

14. Ramamoorthy, S., Leibach, F. H., Mahesh, V. B., Han, H., Yang-Feng, T., Blakely, R. D., and Ganapathy, V. (1994) Functional characterization and chromosomal localization of a cloned taurine transporter from human placenta. *Biochem. J.* **300**, 893–900

15. Burg, M. H. (1995) Molecular basis of osmotic regulation. *Am. J. Physiol.* **268**, F983–996

16. Lang, F., Busch, G. L., Ritter, M., Völkl, H., Waldegger, S., Gulbins, E., and Häussinger, D. (1998) Functional significance of cell volume regulatory mechanisms. *Physiol. Rev.* **78**, 247–306

17. Yancey, P. H., Clark, M. E., Hand, S. C., Bowlus, R. D., and Somero, G. N. (1975) Living with water stress: evolution of osmolyte systems. *Science* **217**, 1214–1222

18. Kurz, A. K., Schliess, F., and Häussinger, D. (1998) Osmotic regulation of the heat shock response in primary hepatocytes. *Hepatology* **28**, 774–781

19. Welch, W. J. and Brown, R. (1996) Influence of molecular and chemical chaperones on protein folding. *Cell Stress Chap.* **1**, 109–115

20. Wettstein, M. and Häussinger, D. (1997) Cytoprotection by the osmolytes betaine and taurine in ischemia-reoxygenation injury in the perfused rat liver. *Hepatology* **26**, 1560–1566

21. Park, E., Schuller-Levis, G., and Quinn, M. R. (1995) Taurine chloramine inhibits production of nitric oxide and TNF-∝ in activated RAW 264.7 cells by mechanisms that involve transcriptional and translational events. *J. Immunol.* **154**, 4778–4784

22. Stapleton P., O'Flaherty, L., Redmond, P., and Bouchier-Hayes, D. J. (1998) Host defense—a role for the amino acid taurine? *J. Parent. Ent. Nutr.* **22**, 42–48

23. Warskulat, U., Wettstein, M., and Häussinger D. (1997) Osmoregulated taurine transport in H4IIE hepatoma cells and perfused rat liver. *Biochem. J.* **321**, 683–690

24. Jaissle, G., May, C. A., Reinhard, J., Kohler, K., Lütjen-Drecoll, E., Zrenner, E., and Seeliger, M. W. (2001) Evaluation of the rhodopsin knockout mouse as a model of pure cone function. *Invest. Ophthalmol. Vis. Sci.* **42**, 506–513

25. Gavrieli, Y., Sherman, Y., and Ben-Sasson, S. A. (1992) Identification of programmed cell death in situ via specific labeling of nuclear DNA fragmentation. *J. Cell Biol.* **119**, 493–501

26. Mansour, S. L., Thomas, K. R., and Capecchi, M. R. (1988) Disruption of the proto-oncogene int-2 in mouse embryo-derived stem cells: a general strategy for targeting mutations to non-selectable genes. *Nature* (*London*) **336**, 348–352

27. Huxtable, J. R. and Lippincott, S. E. (1982) Diet and biosynthesis as sources of taurine in the mouse. *J. Nutr.* **112**, 1003–1010

28. Dumoulin, J.C.M., Van Wissen, L.C.P., Menheere, P.P.C.A., Michiels, A. H., Geraedts, J. P., and Evers, J. L. (1997) Taurine acts as an osmolyte in human and mouse oocytes and embryos. *Biol. Reprod.* **56**, 739–744

29. Dumoulin, J.C.M., Bakker, J. A., Evers, J.L.H., Bras, M., Pieters, M. H., and Geraedts, J. P. (1992) Positive effect of taurine on preimplantation development of mouse embryos in vitro. *Hum. Reprod.* **7**, 403–407

30. Devreker, F., van den Bergh, M., Biramane, J., Winston, R.M.L., Englert, Y., and Hardy, K. (1999) Effects of taurine on human embryo development in vitro. *Hum. Reprod.* **14**, 2350–2356

31. Velazques, A., Delgado, N. M., and Rosado, A. (1986) Taurine content and amino acid composition of human acrosome. *Life Sci.* **38**, 991–995

32. Alvarez, J. G. and Storey, B. T. (1983) Taurine, hypotaurine, epinephrine and albumin inhibit lipid peroxidation in rabbit spermatozoa and protect aginst loss of motility. *Biol. Reprod.* **29**, 548–555

33. Remé, C. E., Grimm, C., Hafezi, F., Marti, A., and Wenzel, A. (1998) Apoptotic cell death in retinal degenerations. *Prog. Retinal Eye Res.* **17**, 443–464

34. Wong, P. (1994) Apoptosis, retinitis pigmentosa and degeneration. *Biochem. Cell. Biol.* **72**, 489–498

35. Lombardini, J. B. (1991) Taurine: retinal function. *Brain Res.Rev.* **16**, 151–169

36. Pasantes-Morales, H., Dominguez, L., Compomanes, M. A., and Pacheco, P. (1986) Retinal degeneration induced by taurine deficiency in light-deprived cats. *Exp. Eye Res.* **43**, 55–60

37. Lima, L. (1999) Taurine and its trophic effects in the retina. *Neurochem. Res.* **24**, 1333–1338

38. Geggel, H. S., Ament, M. E., Heckenlively, J. R., Martin, D. A., and Kopple, J. D. (1985) Nutritional requirement for taurine in patients receiving long term parenteral nutrition. *New Engl. J. Med.* **312**, 142–146

39. Hayes, K. C. and Carey, R. E. (1975) Retinal degeneration associated with taurine deficiency in the cat. *Science* **188**, 949–950

40. Lake, N. (1982) Depletion of taurine in the adult rat retina. *Neurochem. Res.* **7**, 1385–1385

41. Lake, N. and Malik, N. (1987) Retinal morphology in rats treated with a taurine transport antagonist. *Exp. Eye Res.* **44**, 331–346

42. Cocker, S. E. and Lake, N. (1987) Electroretinographic alterations and their reversal in rats treated with guanidinoethyl sulfonate, a taurine depletor. *Exp. Eye Res.* **45**, 977–987

43. van Soest, S., Westerveld, A., De Jong, P.T.V.M., Bleeker-Wagemakers, E. M., and Bergen, A.A.B. (1999) Retinitis pigmentosa: defined from a molecular point of view. *Survey Ophthalmol.* **43**, 321–334

44. Gal, A., Apfelstedt-Sylla, E., Janecke, A. R., and Zrenner, E. (1997) Rhodopsin mutations in inherited retinal dystrophies and dysfunctions. *Prog. Retinal Eye Res.* **16**, 51–79

45. Benini, G., Marconini, C., Wirth, A., and Montagnoli, G. (1988) Is taurine a marker for retinitis pigmentosa? *Ophthalmologia* **197**, 130–135

46. Uma, S. M., Satapathy, M., and Sitaramayya, A. (1983) Decreased plasma taurine levels in retinitis pigmentosa. *Biochem. Med.* **30**, 49–52

Received September 7, 2001; revised October 30, 2001.

Table 1

Body and organ masses from *(taut+/+)* wild-type, *(taut+/-)* heterozygote, and *(taut-/-)* knockout mice.

Body mass and organ mass [g]			
	(taut +/+) mice (n=4)	***(taut +/-) mice*** (n=7–9)	***(taut -/-) mice*** (n=7–9)
Body mass	43 ± 1	41 ± 2	30 ± 1*
Brain	0.44 ± 0.01	0.40 ± 0.02	0.39 ± 0.01*
Heart	0.19 ± 0.01	0.19 ± 0.01	0.18 ± 0.02
Lungs	0.22 ± 0.01	0.24 ± 0.02	0.25 ± 0.01
Liver	2.12 ± 0.17	2.08 ± 0.22	1.79 ± 0.13
Spleen	0.16 ± 0.06	0.18 ± 0.04	0.16 ± 0.03
Right kidney	0.29 ± 0.01	0.26 ± 0.02	0.23 ± 0.01*

Body mass and wet organ mass from 17–18 month-old mice are given. Data are expressed as mean ± SE.
*Significantly different from the *(taut+/+)* wild-type mice (P<0.05).

Table 2

Taurine levels in plasma and tissues of *(taut+/+)* wild-type and *(taut-/-)* knockout mice.

	(taut +/+) mice	***(taut -/-) mice***
	µmol/l	µmol/l
Plasma	673 ± 100	112 ± 18
	µmol/g wet weight	µmol/g wet weight
Liver	9.5 ± 2.1	2.1 ± 1.2
Kidney	6.0 ± 0.9	1.2 ± 0.2
Heart	24.4 ± 2.7	0.6 ± 0.1
Skeletal muscle	32.0 ± 4.9	0.4 ± 0.1
Eye	27.9 ± 12.9	7.1 ± 0.3

Taurine concentrations were measured as described in Materials and Methods. Data are from 2–19 month-old mice each (*n*=5–9), except eye taurine levels are from 12-day-old mice (*n*=3–4). Data are expressed as mean ± SE.

Fig. 1

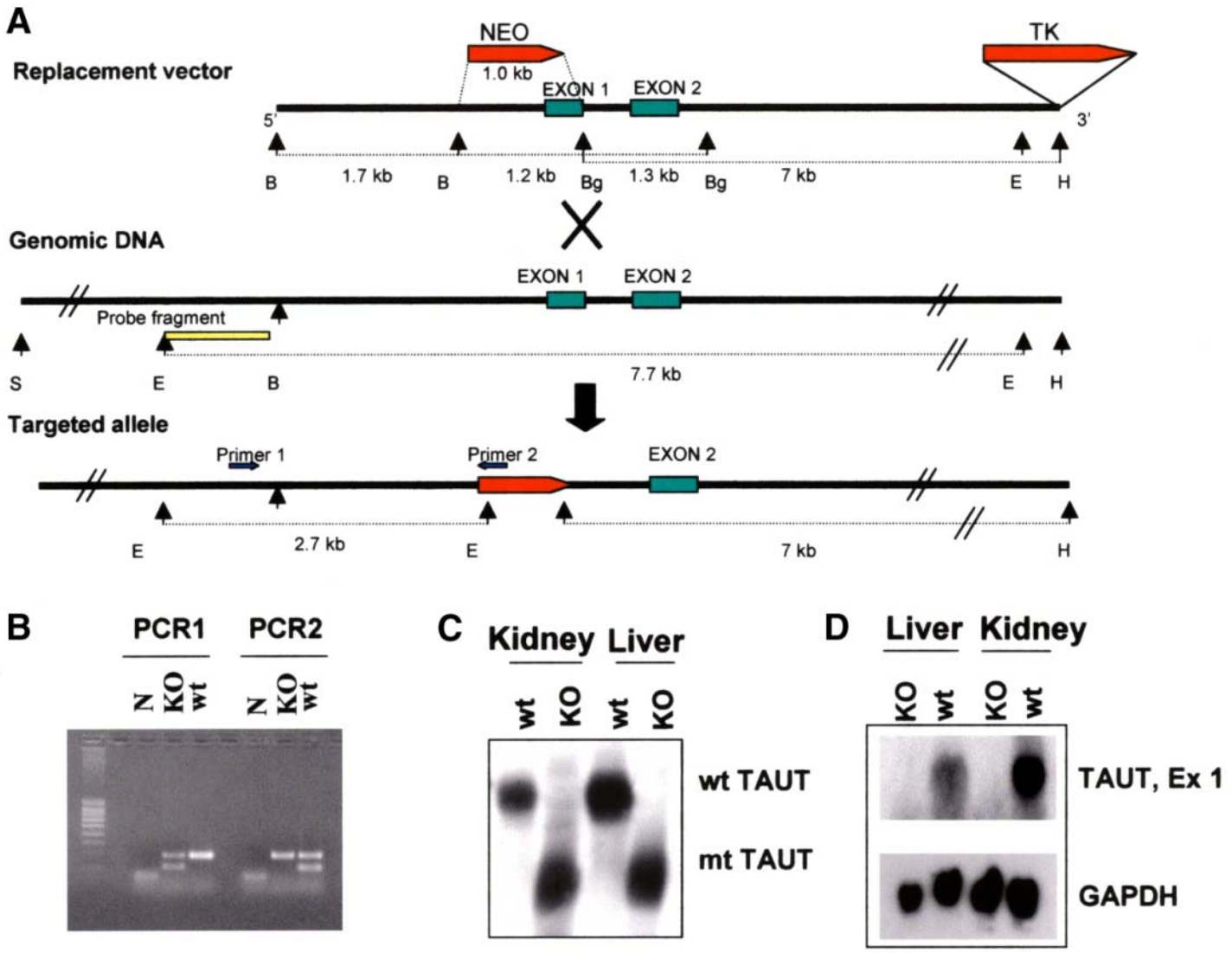

Figure 1. ***Taut*** **gene disruption by homologous recombination. A)** Scheme of the wild-type *taut* locus, the targeting (replacement) vector, and the predicted structure of the targeted *taut* gene. The 5′ external probe used for Southern blot analysis and the size of restriction fragments detected with this probe in the wild-type and targeted alleles are indicated, as well as PCR primers. **B)** Genotyping of the *(taut-/-)* mice. In *(taut-/-)* mice a 117 bp fragment of the targeting construct (PCR1: lower band in lane KO) could be amplified with the primers taut-neo2 and neo2. Exon 1 could not be amplified in *(taut-/-)* mice with the primers TEX25/2 and taut-Ex2r (PCR2: lane KO) but in wild-type mice (109 bp fragment: lower band in lane wt). In all PCR reactions exon 2 is amplified as an internal control (196 bp fragment: upper bands in lanes wt and KO). **C)** *In vitro* translation/transcription of the TAUT cDNA isolated from wild-type and *(taut-/-)* mouse. In *(taut-/-)* mice a truncated protein can be translated from the cDNA. **D)** Northern blot analysis of wild-type and *(taut-/-)* mice using a probe for exon 1 of the TAUT gene and GAPDH. The expression of *taut* exon 1 is observed in the wild-type mouse only. **B**, BamHI; **Bg**, Bgl II; **E**, EcoRI; **H**, HindIII; **S**, SacI; **N**, negative control; **KO**, *(taut-/-)* mouse; **wt**, *(taut+/+)* mouse.

Fig. 2

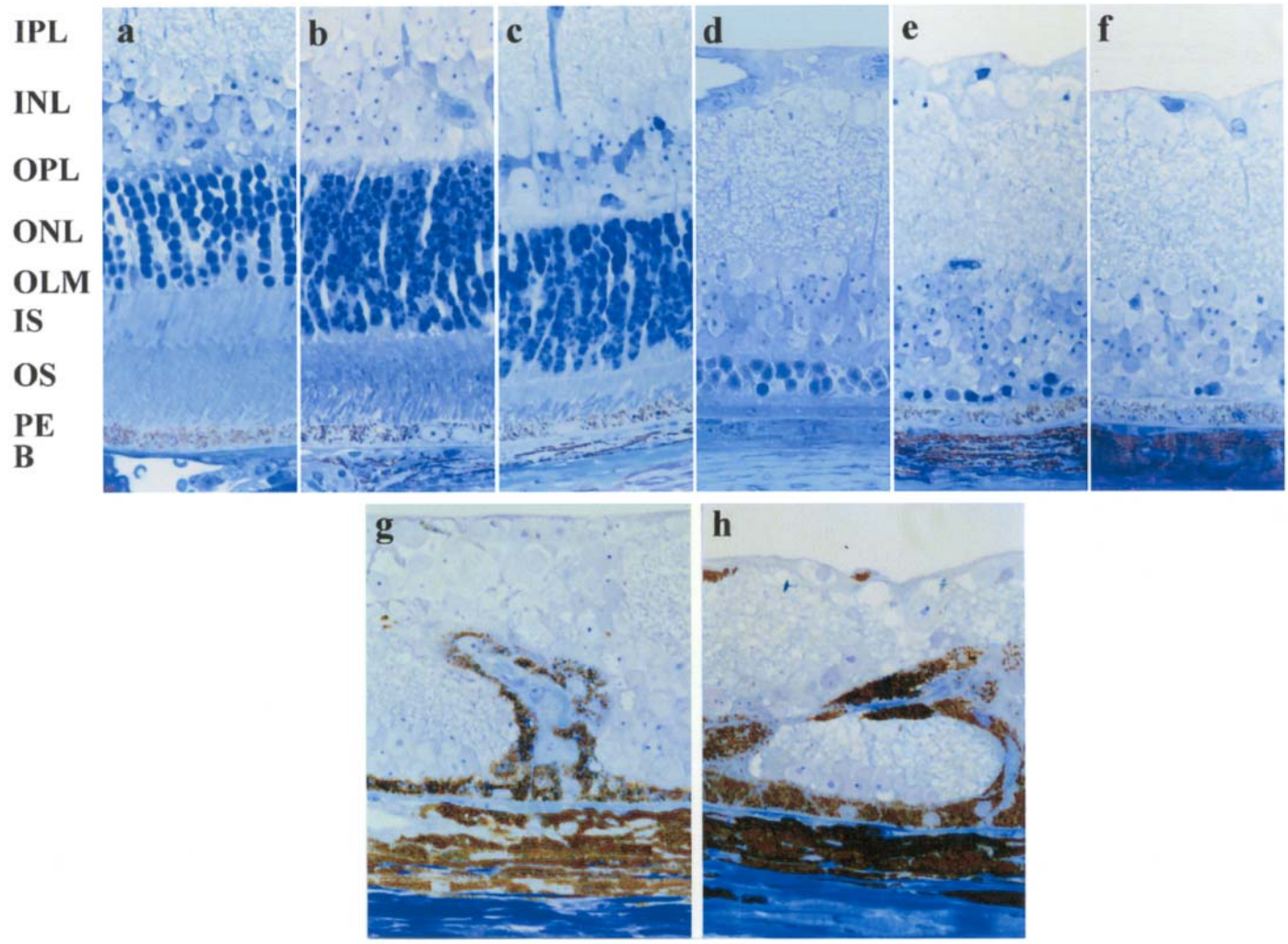

Figure 2. Retinal morphology of wild-type and *(taut-/-)* mice. a, b) Retinas of wild-type (*taut*+/+) mice at 17 months **(a)** and at postnatal day 14 (b). **c–h)** Retinas of (*taut-/-)* mice at postnatal day 14 **(c)**, 1 month **(d)**, 2.5 **(e)**, 4 **(f)**, 9 **(g)**, and 13 months **(h)**. Toluidine staining of semithin sections; all micrographs at 450×. No nuclei of the ONL were discernible in age-matched (*taut* -/-) mice beyond an age of 2.5 months. Note that in **Figure 2a–f** the layers of the retina are set to the PE, so that reduction of the ONL becomes readily evident. **Figure 2g** and **h** are set to the membrane of Bruch. **IPL**, inner plexiform layer; **INL**, inner nuclear layer; **OPL**, outer plexiform layer; **ONL**, outer nuclear layer (photoreceptor nuclei); **OLM**, outer limiting membrane; **IS / OS,** inner / outer segments of photoreceptors; **PE**, pigment epithelium; **B,** membrane of Bruch.

Fig. 3

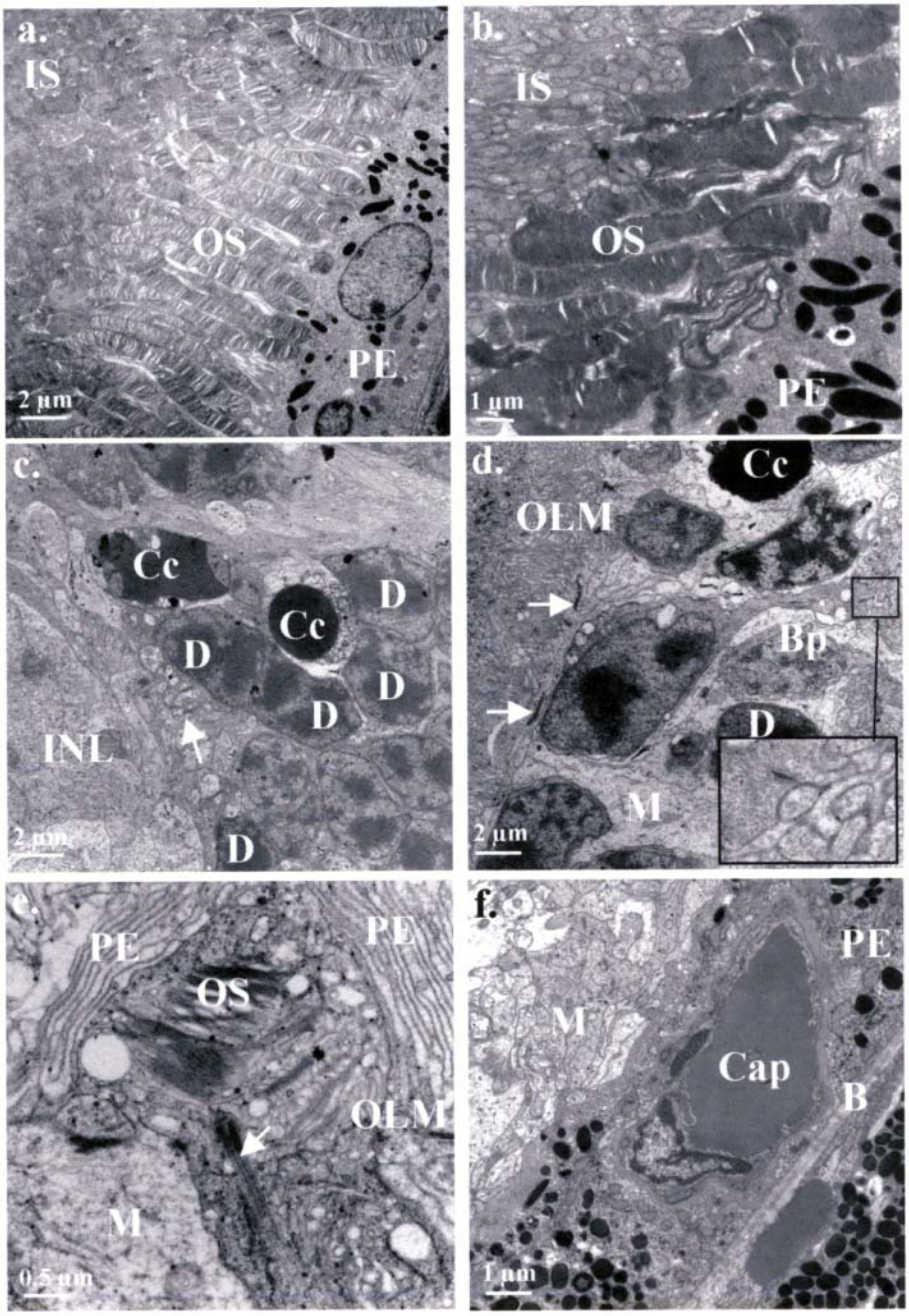

Figure 3. Retinal morphology of wild-type and *(taut-/-)* mice (electron microscopy) a) Retina of wild-type mouse of 14 days: outer segments (rods) at the pigment epithelium (PE), which rests on Bruch's membrane. **b)** Inner and outer segments at the PE in (*taut* -/-) mouse of 14 days. Disk arrangement is disrupted in many of the outer segments but inner segment structure is almost normal, as is that of the PE. **c)** Inner region of ONL (at the right) and INL (at the left) in 14 day old (*taut* -/-) mouse. Nuclei of two photoreceptor cells have highly condensed chromatin (Cc), several neighboring cells have abnormally dark nuclei (D). Synapses can be seen in the outer plexiform layer (arrow). **d)** ONL with PE (at the left) and outer plexiform layer (at the right) in (*taut* -/-) mouse of 1 month. Remaining nuclei of photoreceptor cells show various stages of degeneration and Muller cell processes between them are swollen. Outer limiting membrane at PE (no pigment in this animal) is still intact. Inset: detail of ribbon synapse. **e)** Remnants of outer segment surrounded by microvilli of PE in (*taut* -/-) mouse of 1 month. Disrupted disks and supporting cilium (arrow) can still be identified. The Muller processes are distended. **f)** PE between Bruch's membrane and processes of Muller cells in (*taut* -/-) mouse of 13 months. The continuity of the retinal PE is interrupted by a capillary surrounded by basal lamina. **ONL** = outer nuclear layer; **OS / IS** = outer / inner segments; **PE** = pigment epithelium; **B** = Bruch's membrane; **Cap** = capillary; **D**= dark nuclei; **OPL** = outer plexiform layer; **M** = Muller cell process; **Cc** = condensed chromatin.

Fig. 4

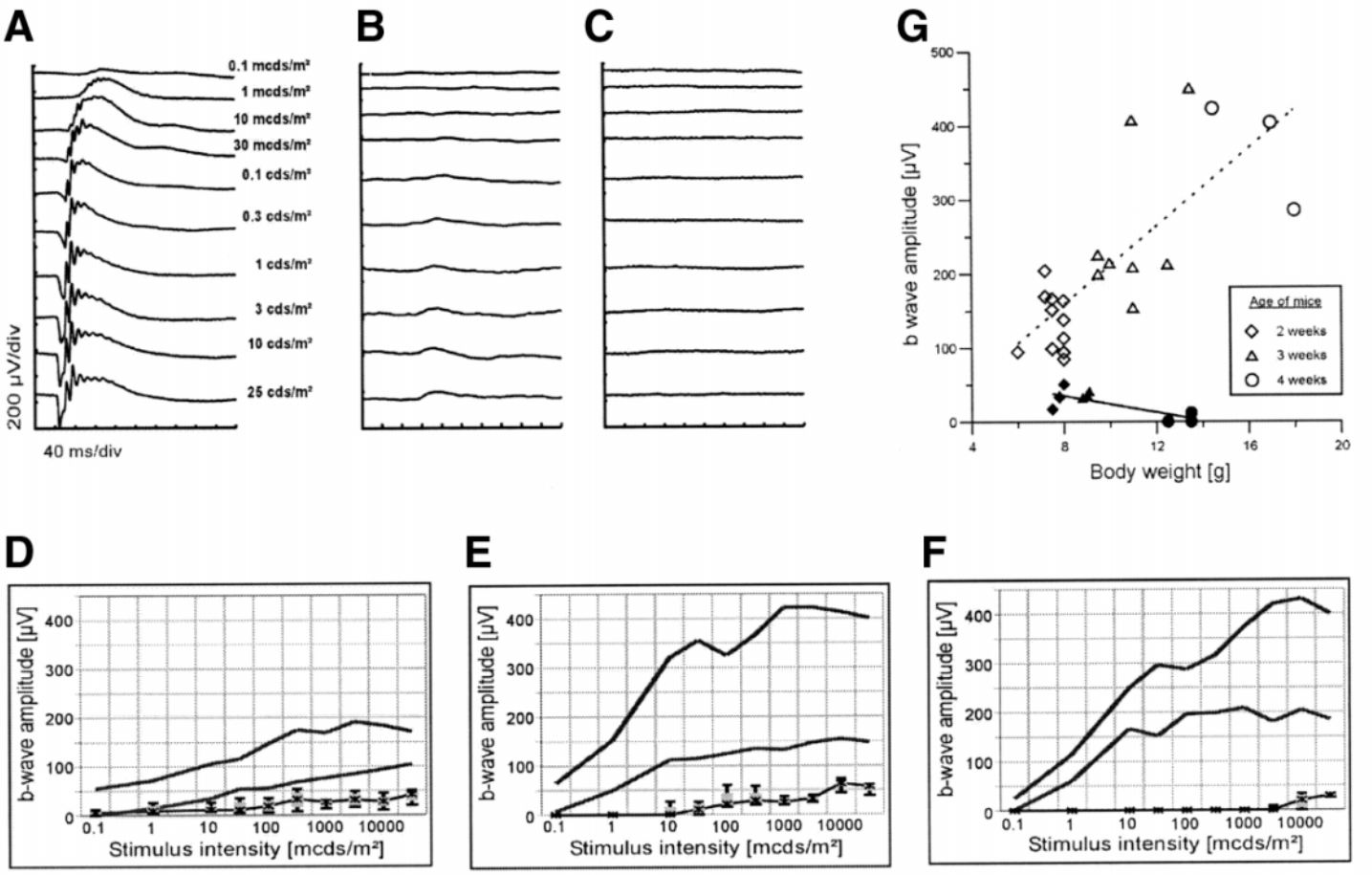

Figure 4. Retinal function in (*taut-/-*) mice is progressively impaired with age. A–C) Scotopic single flash ERG intensity series for adult control **(A)** and (*taut -/-*) mice at 3 **(B)** and 6 **(C)** weeks postnatally. Stimulus range: 0.0001 (top trace) to 25 cd*s/m² (bottom trace). Shown are exemplary traces from individual animals. (*taut-/-*) mice at ages between 2 and 4 weeks revealed some small, but distinct remaining electrical activity, whereas there was no sign of light-induced retinal responses beyond the age of 6 weeks. **D–F)** Amplitude-vs.-intensity functions of developing (*taut-/-*) and control mice at 2 **(D)**, 3 **(E)** and 4 **(F)** weeks postnatally. In each graph, the normal range lies between the top wide line, denoting the 95% quantile, and the bottom wide line, indicating the 5% quantile of the control group. The box plots show the results obtained with (*taut-/-*) mice, depicting the median (cross; connected by black line), the 75% and 25% quantile corresponding to top and bottom end of the box, and the 95% and 5% quantile corresponding to top and bottom end of the bar. It is obvious that the ERG amplitudes of taut-deficient animals lie below the normal range at all ages tested. Whereas the controls show the expected developmental increase from week 2 towards almost adult values at week 4, there is no significant increase between week 2 and 3 in the knockouts, but a distinct loss of ERG activity from week 3 to 4. The double-peaked shape of the curves **(D, E)** suggests that both rods and cones have some remaining function. **G)** Body weight is not a major factor for the ERG reduction. Shown is the b-wave response to a 3 cds/m² stimulus vs. body weight of individual animals obtained at 2 to 4 weeks postnatally. Open symbols indicate control animals, and filled symbols (*taut -/-*) mice. The ERG of controls of comparable weight—regardless of the age—was much larger in all cases.

Fig. 5

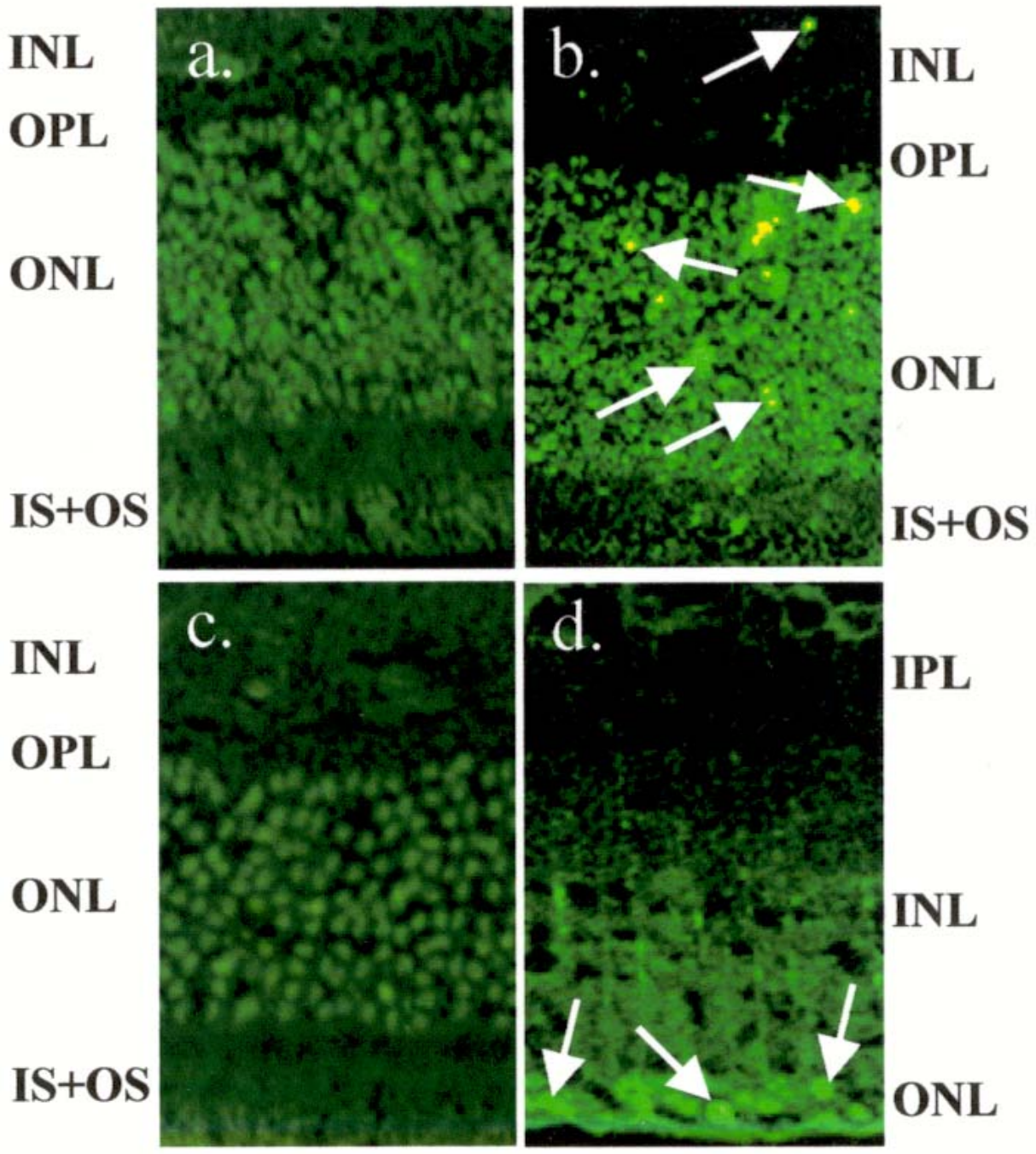

Figure 5. Fluorescence microscopy of photoreceptor apoptosis in (*taut* -/-) mice. At postnatal day 14 (P14), wild-type (*taut* +/+) mice (**a**) show a retinal differentiation with inner and outer segments (IS + OS), outer (ONL) and inner nuclear layer (INL). Retina of 6-week-old wild-type mouse is shown in (**c**). Many condensed (fluorescent) nuclei of apoptotic cells are found in ONL of (*taut* -/-) mice at P14 (b) and after 6 weeks (d) (see arrows). For abbreviations, see legend **Figure 3**.